

BORON AND PHOSPHORUS IMPLANTATION IN SILICON

by 4589

J. DAVID SCHNEIDER

B. S., University of Missouri-Rolla, 1968

-

A MASTER'S THESIS

submitted in partial fulfillment of the

requirements for the degree

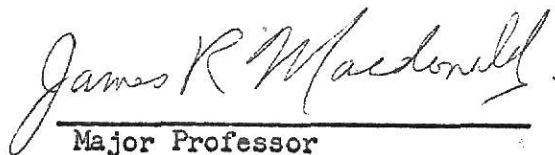
MASTER OF SCIENCE

Department of Physics

KANSAS STATE UNIVERSITY
Manhattan, Kansas

1970

Approved by:


Major Professor

ILLEGIBLE DOCUMENT

**THE FOLLOWING
DOCUMENT(S) IS OF
POOR LEGIBILITY IN
THE ORIGINAL**

**THIS IS THE BEST
COPY AVAILABLE**

LD
2668
T4
1970
S3715
C.2

11

TABLE OF CONTENTS

	Page
INTRODUCTION	1
BACKGROUND	3
HISTORY	19
PREPARATION OF CRYSTALS	22
IMPLANTATION APPARATUS	27
TEST PROCEDURE	35
RESULTS	40
CONCLUSION	58
ACKNOWLEDGMENT	61
REFERENCES	62

LIST OF TABLES

Table	Page
I. Summary of Results on All Implanted Wafers	46

LIST OF PLATES

Plate	Page
I. Plots of the atomic and electronic energy loss as a function of energy for phosphorus and boron ions in silicon	6
II. Concentration profile of ^{32}P ions implanted at 110 keV along the $\langle 110 \rangle$ direction in single crystal silicon	10
III. Qualitative shape of energy bands in the region of a p-n junction, with and without reverse bias	18
IV. Mount used for positioning the silicon wafers during implantation	25
V. Schematic of a typical implantation system	29
VI. Gas handling system used to provide boron and phosphorus for the ion source	31
VII. Effect of fusing current on the current-voltage characteristics between front and rear of a typical implanted wafer	43
VIII. Typical current-voltage characteristics for a device with evaporated contacts	51
IX. Electron micrographs of both implanted and unimplanted regions on a heavily implanted crystal	55
X. Electron micrographs taken from surface of crystal heavily doped with phosphorus, showing massive damage	57

INTRODUCTION

Recent review articles by several authors (e.g. Gibbons, 1968; Dearnaley, 1969) have pointed out the versatility of the ion implantation technique as a valuable tool for altering, in a controllable manner, the physical, chemical, and electrical properties of a solid. Ion implantation seems especially adaptable to the doping of semiconductors, where the interesting electrical behavior is caused by extremely small concentrations of impurities with variations over very small regions of the crystal. In diffusion technology, an oxide layer can present serious problems, but it is possible to implant through a thin oxide layer. The idea of implanting one type of dopant ion into an opposite type semiconductor substrate seems advantageous for several reasons. Implantation allows doping at levels much more shallow than those possible by diffusion techniques. Also the doping can be more uniform over a large surface area. Damage produced by bombarding ions will introduce many trapping centers for the charge carriers, but in general this damage can be repaired by annealing at temperatures (300-900 °C) lower than those normally needed (800-1200 °C) to introduce impurities by diffusion.

Much of the attractiveness of implantation stems from the fact that it is a non-equilibrium process, which means that the maximum local concentration of the dopant ion species is independent of the chemical solubility. In addition the dopant ions may be of any species which can be produced in an ion source. The large degree of control which the researcher has over the ion energy, as well as his control over substrate parameters such as temperature and orientation, affords him a high degree of regulation over the penetration depth and concentration profile of the

implanted ions.

The use of ion implantation to fabricate position sensitive particle detectors offers some attractions over the present methods. Currently the diode structure of these position sensitive devices is produced by a surface barrier type diode on the front surface of a thin crystal. The rear surface is then thinly plated with a metal to provide the uniform resistive layer necessary for yielding a signal sensitive to particle position.

Laegsgaard et al (1968) describe a method of producing these detectors in which the impurities introduced by implantation provide both the p-n junction and the layer of uniform resistivity on the front surface. The ion implantation technique produces devices that are more rugged than those using a thin metal film. The surface film, unless suitably protected, will be susceptible to abrasion and contaminants such as water vapor in the ambient. An implanted region, since it is beneath the surface, can be expected to be more resistant to such effects. By suitably choosing the levels of doping, the conductivity across the active region can be varied within wide limits.

Because of the fragility of the surface barrier structure, any usable diode thus fabricated must be encapsulated for protection. Since this protective structure is usually formed from epoxy or other plastic material, it is often not possible to heat the entire unit in order to anneal out the radiation damage produced by prolonged use of the detector. With the more rugged implanted diode it should be a simple matter to demount the crystal and reanneal to repair most of the damage produced in use.

BACKGROUND

Before considering the specifics of ion implantation, a brief description will be given of the processes involved in the stopping of energetic ions in matter. Both elastic and inelastic interactions between the incident ion and atoms within the target contribute to the stopping of the moving ion. At larger velocities it is found that electronic excitations absorb energy from the moving ion and thus give rise to an electronic stopping power. When the ionic velocity is greater than the electron velocity in the K-shell, the ion has a good probability of being stripped of all its electrons. Early theoretical work for this condition was done by Bohr (1913), Bethe (1930), and Bloch (1933). Significant nuclear excitations occur only at energies well above those normally used for implantation so their contribution can be ignored.

At some intermediate velocities, when the ion is no longer fully stripped, an estimate of the stopping power may be made by assuming an effective charge on the ion. This effective charge will be dependent upon the number of positive charges in the nuclei of both the incoming ion and target atoms, as well as the velocity of the ion. Northcliffe (1963) has considered the region of validity of this Bethe-Bloch formula. A somewhat different approach outlined by Firsov (1959) views each binary collision as an overlap of electronic orbitals. His treatment is adaptable to both low and intermediate velocities.

At lower velocities screened coulomb forces between nuclei give rise to Rutherford-type scattering. Electronic effects, giving a stopping power in this region approximately proportional to ion velocity, (Lindhard, et al 1961) become of less importance in stopping the projectile than are the

energy losses due to recoiling atoms. Theoretical calculations of this elastic stopping power rely upon the choice of an appropriate screened nuclear potential. Both the inverse power law and the Thomas-Fermi potentials were considered in the detailed treatments of stopping by Lindhard et al, (1963). Figures 1 and 2 are plots of the elastic and inelastic stopping powers for phosphorus and boron ions in silicon. These data are taken from tables presented by Johnson and Gibbons (1969). Their calculations follow the method of Lindhard, hence are appropriate only for amorphous targets.

With some understanding of stopping powers, it becomes meaningful to speak of ranges of ions within a solid. These ranges may be defined in various ways, but will always refer somehow to the distance travelled by an ion within the crystal before coming to rest somewhere in the lattice. The term total range is self-explanatory, being the total distance travelled by the ion in coming to rest. A more useful term is projected range, which refers to the total range projected onto the initial direction of the incident ion. Because no two ions will follow exactly the same path through the crystal or will suffer exactly the same sequence of collisions, there will be a statistical spread in the ranges of the ions, leading to range distributions. The mean square fluctuation in ion range is usually called range straggling.

The first published theoretical work on range energy relations, projected ranges, and straggling in ion ranges was that of Lindhard et al, (1963). Their work was applicable to only amorphous targets in which the collision events were totally random. They made estimates of stopping powers, and from these used numerical integration techniques to predict ranges. Using the methods outlined by Lindhard et al, Gibbons and Johnson

**THIS BOOK
CONTAINS
NUMEROUS PAGES
WITH DIAGRAMS
THAT ARE CROOKED
COMPARED TO THE
REST OF THE
INFORMATION ON
THE PAGE.**

**THIS IS AS
RECEIVED FROM
CUSTOMER.**

EXPLANATION OF PLATE I

Figure 1 is a plot of the two predominant energy loss mechanisms of phosphorus ions in silicon as a function of energy of the incident phosphorus ions.

Figure 2 is a similar plot of the electronic and atomic energy losses of boron ions in silicon.

PLATE I

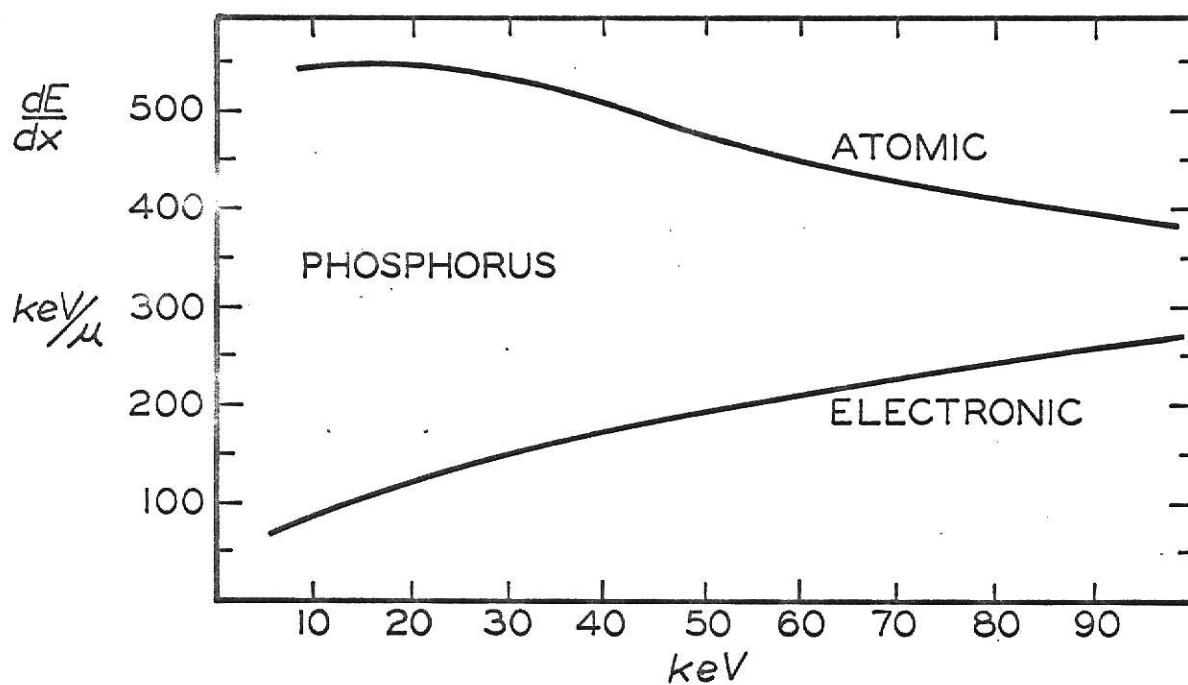


FIG. 1

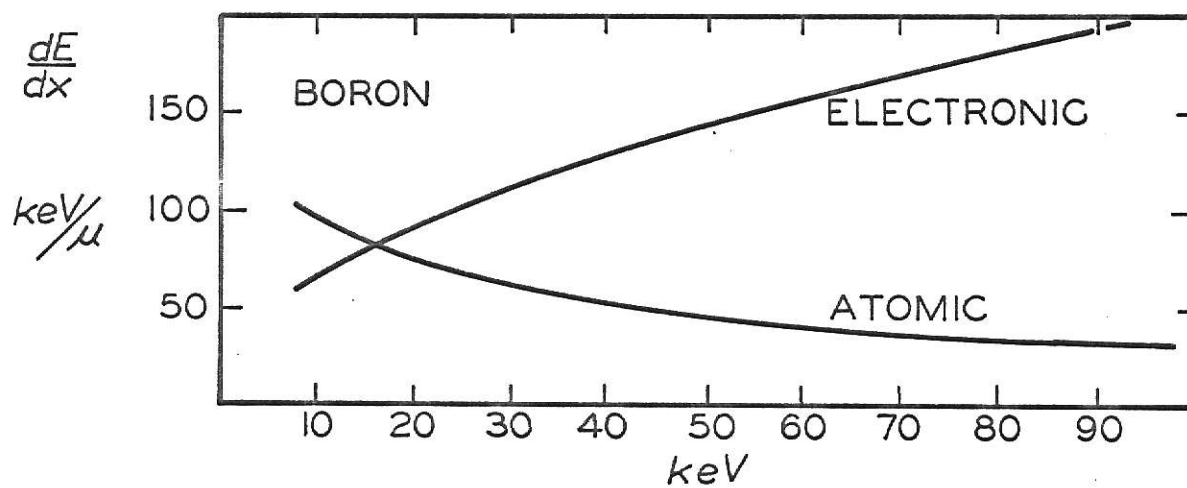


FIG. 2

have published tabulated values for ranges of numerous ions in a variety of target materials. Experiments by Powers et al (1962) and Kleinfelder et al (1968) have shown that the predictions based on Lindhard's work agree well with observations, if the crystal is so oriented or damaged that channeling effects are negligible. Crowder et al (1969) have reported that profiles in non-channelled directions can be characterized by nearly the theoretical Caussien distributions with small tailing effects on the deeper side.

For single crystals such as silicon, Alvager et al (1962) found that many ions are steered down low index directions. Especially when the beam is initially incident along one of the low index directions within the crystal, a fraction of the ions will suffer only small angle scattering as they are channeled, never experiencing close encounters with the atoms of the host material. Hence channeled ions may have anomalously large ranges. Apparently the first analytical calculation of channeling was made using Bohr and Born-Mayer potentials by Lehmann and Liebfried (1963). The concept of a string or row of atoms and an associated continuum potential based on the Thomas-Fermi atomic model was proposed by Lindhard (1965). From this treatment it is possible to determine a critical angle for scattering. This is the maximum angle off a low index direction, for given ions at given energy, at which those ions can still be channeled through the crystal. In spite of the fact that interatomic potentials are believed to be well understood, there is at present no theory which can accurately predict the ranges of channeled ions. Interatomic potentials useful in channeling calculations have been proposed by Thomas (1927) and Fermi (1928). Their model is used to approximate the screened potential for atoms when the separation distance is larger than the Bohr orbit. Modifications of their method have since been devised, and many of these, including numerical techniques for accurate

determination of collision parameters, have been summarized by Testerman (1969). Because of the difficulty in properly integrating the stopping powers for all orientations of the crystal lattice, and in including the dechanneling contributions to the range distributions, theoretical predictions of ranges of channeled ions remain inaccurate.

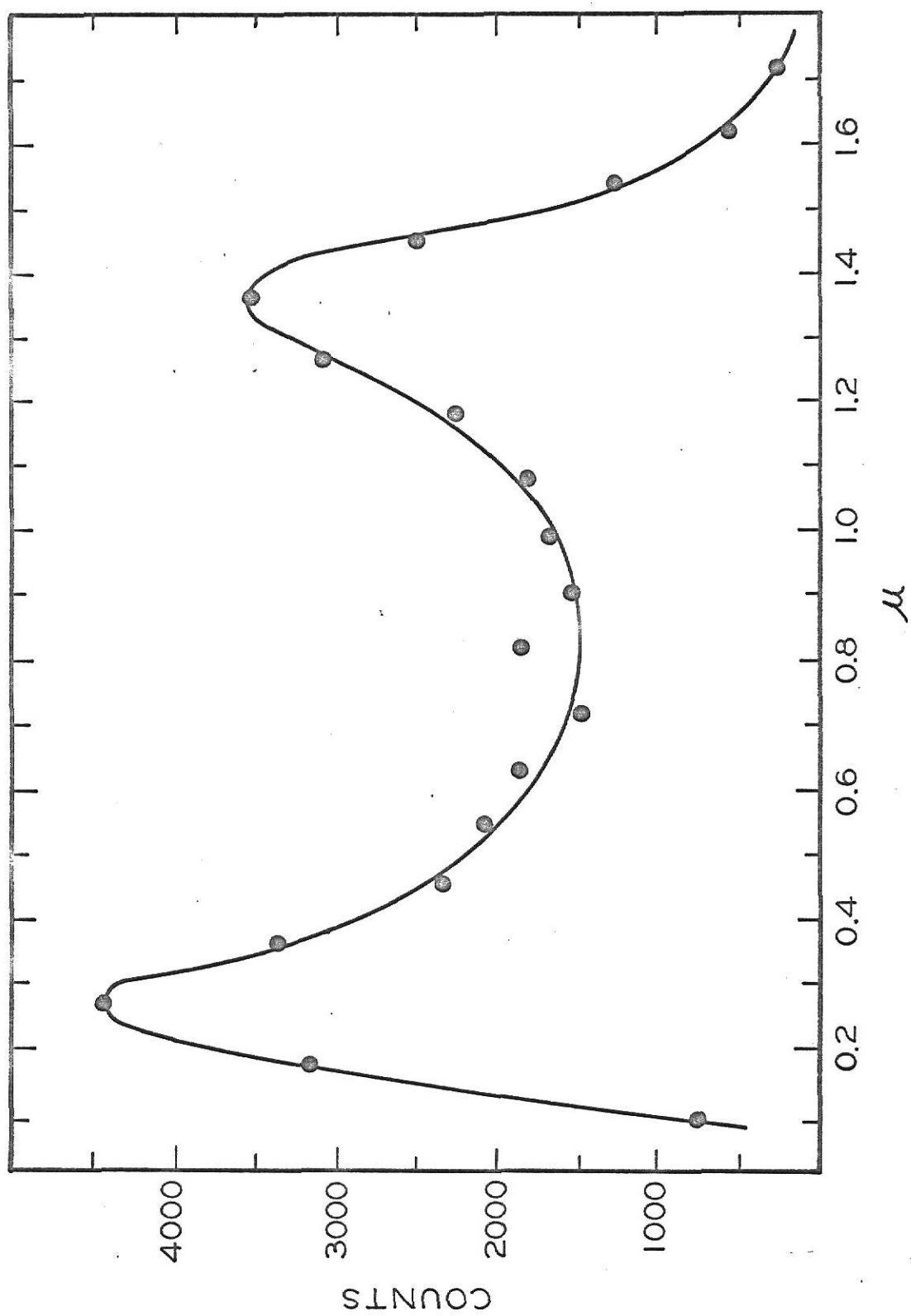
Several methods have been devised to measure ion ranges. Probably one of the more precise techniques is that of anodic stripping, outlined by Davies et al (1960). This method and adaptations of it (Dearnaley, 1969) are most appropriate for use with radioactive tracers. By this means the radioactivity present in successively removed layers gives a determination of differential range distributions of the implanted radioactive species. A profile of ^{32}P ions in silicon measured in this manner is shown in Plate II. This is an example of the impurity profile obtained when the crystal is so oriented that ions are incident in a channeling direction. The peak closer to the surface is due to the non-channeled ions, and is at the approximate position predicted by estimates for amorphous targets. The maximum expected range of channeled ions corresponds roughly to the position of the deeper peak. Ions dechanneled sometime during the stopping process are believed to account for the nearly filled-in region between the two peaks.

In semiconductor materials other methods may be utilized to determine the impurity distribution. One technique (Kleinfelder et al, 1968) involves exposing and staining the p-n junction produced by the implantation of a donor or acceptor type ion species into the opposite type substrate. Another method is that of repeatedly measuring the sheet resistance as thin layers are removed from the crystal surface. However both these methods measure only the concentration profile of electrically active dopant ions. This point is significant because generally only a fraction of the implanted impurity ions

EXPLANATION OF PLATE II

The relative beta activity from ^{32}P atoms in successively removed thin layers from the implanted silicon surface. These data are from Dearnaley et al (1968) and are taken from 110 keV ^{32}P ions implanted at room temperature along the $\langle 110 \rangle$ direction to a dose of 5×10^{12} ions/cm².

PLATE II



are electrically active (Crowder et al, preprint of 1969).

Eriksson et al (1967) have described how the orientational and energy dependence of backscattered 1 MeV protons and helium atoms may be used to determine the lattice disorder and location of dopant ions within the crystal. In this method, the less massive probe ions are sent down low index crystallographic directions in the lattice. A precise analysis of the angular and energy dependence of the backscattered ions can then locate the impurity ion, as well as give an indication of the amount and extent of the lattice damage.

Damage caused by the impinging ions may take several forms. Each incoming ion will produce a number of vacancies by removing host atoms from their normal positions within the lattice. Many other atoms from the host crystal will be displaced slightly from normal positions. A few of the stopped ions will have replaced the normal atoms at their regular lattice sites. Many atoms will reside in interstitial positions, these being both the displaced host atoms and the great majority of incoming ions which come to rest at non-lattice sites.

Any form of lattice damage produced by ion bombardment is usually termed radiation damage. Since defects in a normal structure produce abnormal stresses within the crystal, the energies associated with this lattice distortion will be increased over that of the unmodified lattice. There will be a tendency for many of these individual defects to cluster as the lattice seeks to return to a lower energy state. Large scale dislocations may also result from the massive damage. The clustering of these defects may be used to advantage in some instances. After prolonged bombardment with ions, these clusters can be made to overlap, thus producing an essentially amorphous region in the crystal (Mazey, Nelson and Barnes, 1968). All ions

incident upon such a region will be unable to see any channels along low index directions. Hence the ranges of these ions can be expected to follow very nearly the theoretical predictions for amorphous targets. As measured by helium atom backscattering, Davies et al, (1967) have found associated with the disordered region a "milky" appearance of the surface. Nelson and Mazey (1968) state that the threshold dose at which this visible damage occurs is dependent upon crystal temperature during implantation. By their measurements, this cloudiness seems to appear in room temperature silicon at a dose of about 10^{14} ions/cm².

The extensive radiation damage is regarded as the primary disadvantage for ion implantation, as it is usually desired to retain a crystalline structure which is as near normal as possible, with the introduced impurity ions residing in substitutional sites within the lattice. Since typical activation energies for migration in crystals are 0.5 eV for vacancies and 0.2 eV for interstitials (Dearnaley, 1969), at all but the lowest temperatures there will be a tendency for some reordering of the lattice. This reordering can be greatly enhanced by annealing the crystal, a process of heating the crystal to allow thermal vibrations to assist in the restoration of the normal structure. Care must be taken to control the environment and to limit the temperature during annealing to prevent significant diffusion of the impurity atoms.

In the usual process, annealing is performed in a separate step, following the implanting process; however in many instances the crystal is held at an elevated temperature to allow significant reordering even as the ions are being injected. In the final distribution, more of the ions will be found to have been channeled when the damage is thus kept to a minimum. If, on the other hand, it is desired to maximize damage to

minimize channeling effects, some researchers (Crowder et al, preprint of 1969) have held the specimen at low (liquid nitrogen) temperatures while implanting. They have found that this is a useful procedure to enhance the subsequent electrical activity of the implanted boron.

In most work with ion-implanted silicon, the greatest concern is with electrical activation of the impurities, rather than with only the restoration of the lattice structure. There seem to be different stages in the range of annealing temperatures at which different phases of damage repair occur and at which impurities are rendered electrically active. These many stages in the annealing have been discussed in detail (van Bueren, 1960). Much of his work was done with metallic crystals and is perhaps not directly applicable to silicon. Dearnaley (1969) has stated that in silicon the annealing is characterized by the interaction of simple point defects with other imperfections, principally impurity atoms, and the behavior is strongly dependent upon the impurity content of the material.

Some reordering of the lattice and migration of defects will occur at lower temperatures, but true recrystallization seems to begin at about 600 °C (Davies et al, 1967). Analysis by electron microscope will indicate many dislocation loops even after treatment at this temperature. At the stage where electron microscopy shows no damage, electron paramagnetic resonance, in which transitions are induced between the Zeeman levels of a paramagnetic defect in the crystal, can be used to locate remaining damage (Watkins et al, 1959).

Since the primary purpose of this study was to investigate the feasibility of making junction type particle detectors by ion implantation in silicon, it is appropriate to discuss briefly the theory associated with a p-n junction. The p-n junction is formed at the interface between

two regions in a single piece of semiconductor; one region doped predominantly with acceptor, the other with mostly donor impurities. In silicon, donor impurities are those elements which have five electrons in the outer orbital. Since only four electrons are needed to complete the normal silicon type covalent bond, the fifth electron is then relatively free to move about the lattice. Acceptor type impurities, on the other hand, are those atoms with only three electrons in the outer orbital, thus only these three electrons are available for bonding in the silicon bond. This absent electron, or hole, is then relatively mobile within the crystal structure.

The electrical properties of a p-n junction will differ from those of normal extrinsic material. As soon as the junction is formed, by diffusion, implantation or otherwise, a net diffusion current flows from one type material to the other. This leads to an electrostatic potential difference across the junction even at equilibrium. Because of the higher volume concentration of electrons in the n-type material, many will diffuse into the p-type region. For the same reason, holes move across into the n-type material. After having crossed the junction, many of these carriers recombine with the majority carriers in the new host material. Since very few of the recombined carriers are replaced by thermal excitation from lower energy levels, the region of the junction becomes deficient in carriers, and is known as the depletion region. Due to the recombination process, ions located in the depletion region are no longer neutralized by an equal number of carriers of opposite sign. The net result is that in the depletion region, there is a net positive charge on the n side of the junction, and a net negative charge on the p side. A potential difference giving rise to an electrical field is thus generated in the junction area. This electric

field may have a local value as high as 2×10^4 volts/cm (Smith, 1959).

The form of the energy levels around the junction is shown in Fig. 3.

From the Figure it can be seen that the potential difference thus generated must be somewhat less than the energy band gap of the solid.

The creation of a pair of carriers, electron plus hole, requires an average of about 3.6 eV in silicon (Pehl et al, 1969), so the number of carrier pairs produced by a particle being stopped within the silicon will be given approximately by $E/3.6$, where E is the energy of the incident particle in eV. The exact number of carriers pairs produced will not be known because of the fluctuations and uncertainty in the energy required in an average carrier pair creation.

The incident ions create ion pairs within the silicon lattice by several mechanisms. Ion pairs may be produced directly, each creation taking about 3.6 eV from the moving ion. More frequently, the high velocity projectiles dislodge host atoms, setting them in motion through the lattice. These secondary particles are then the most instrumental in forming ion pairs. In all collisions in which less than about 3.6 eV of energy is transferred, there will not be sufficient energy to form another ion pair. Energies from all those low-energy transfer collisions must be dissipated by phonons in the lattice. The statistical spread resulting from the uncertainty of the exact mechanism of formation of these secondary projectiles and their subsequent energy loss then gives rise to a fluctuation in the average number of ion pairs produced. Since there is an obvious correlation between number of carrier pairs and charge transferred in the external circuit, there can then be derived a direct relation between transferred charge and incident particle energy.

The charge generated within the semiconductor must be collected before

opposite type carriers can recombine or be caught in traps. An electric field may be used to "sweep up" the generated carriers before a significant number recombine. The electric field at the depletion region serves this purpose ideally. An important feature of a p-n junction is that a reverse bias may be applied. The effect of this reverse bias (which is the process of using an external emf to make the n type material positive with respect to the p type) is to further enhance the formation of a wider depletion region and to further reduce the number of current carriers present within that region. The effect of this applied bias on the electron energy level is shown in Fig. 4.

Application of this reverse bias will have three desirable effects upon the capabilities of the detector. First, it will, by decreasing the number of carriers within the depletion region, decrease the conductivity and hence reduce the ambient current which gives rise to noise in a detector. Since the conductivity of the depletion region is many times lower than that of the bulk, almost the entire applied potential must occur across that depletion region. Increasing the applied voltage will increase the efficiency of charge collection, decrease the charge collection time, and also decrease the variation in actual charge collected, for there will be more force on the carriers within the region. In widening the depletion region, that volume of the crystal which is most responsive to detection of energy loss processes will be increased. If this depleted region may be made to extend nearly to one surface of the crystal, the window of the detector, that region which is virtually unresponsive to energy loss processes because charge collection from ion pairs is so inefficient there, will be reduced. Thus, application of reverse bias should lead to more efficient collection of generated charges, as well as shorter collection times.

EXPLANATION OF PLATE III

Figure 3 shows the relation of the Fermie level to the conduction and valence bands in a p-n junction at equilibrium.

Figure 4 shows the shift in the Fermi level when a reverse bias is applied to the junction.

PLATE III

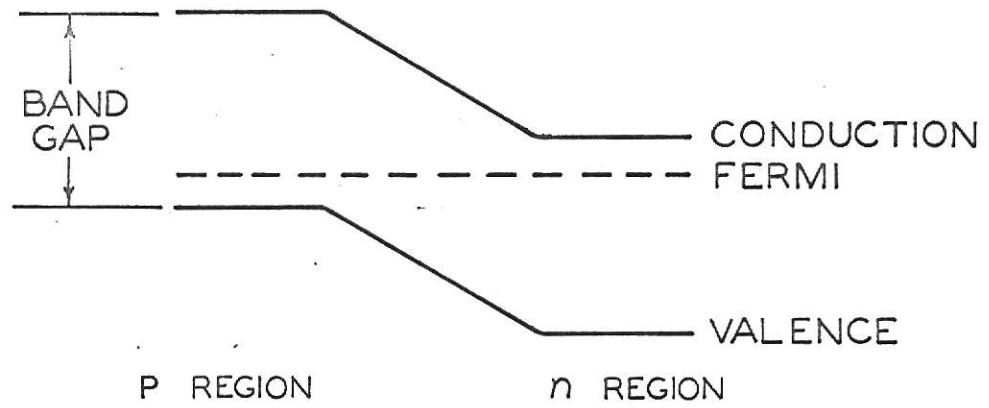


FIG. 3

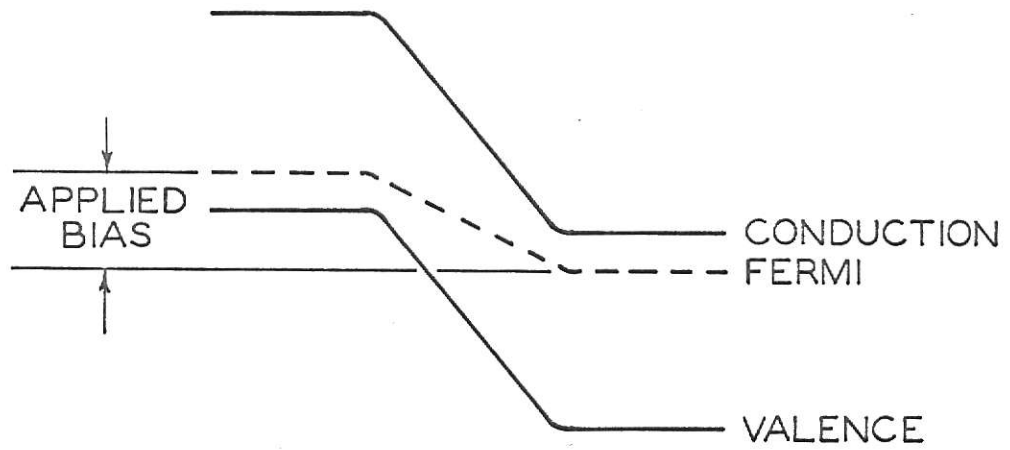


FIG. 4

HISTORY

The history of ion implantation is very short indeed. In 1952 Russell Ohl at Bell Labs bombarded point contact silicon junctions with energetic heavy ions and observed some doping effects, which are believed to have been due mainly to the introduced damage centers. The junctions thus bombarded were observed to be photosensitive. A difference between damaging and doping effects of implanted ions was observed first by Bredov et al (1960), who noted a difference between the use of oxygen and nitrogen ions as dopants. Early patents on the ion implantation process were granted to Ohl (1956), Shockley (1957), and Moyer (1958). From their reports, it is obvious that both Shockley and Moyer were aware of the possible need to anneal after implantation to repair much of the introduced damage.

Rourke et al (1961) implanted group III and IV elements into silicon at about 10 keV., but failed to report on diode characteristics. The fact that implanted phosphorus had a doping effect similar to introduction of the same impurity by diffusion was shown by Alvager and Hansen (1962). They were successful in producing diodes for use as nuclear particle detectors by implanting phosphorus ions, then annealing at 600 °C. The concept of channeling in single crystals was recognized by 1963. At about this same time interest in the implantation technique was beginning to grow rapidly. Earlier devices capitalized on the fact that implantation could produce a uniform concentration of dopant atoms in a very thin layer near the surface. This feature proved useful in making particle detectors with very thin windows, and solar cells. King et al (1965) report the production of implanted solar cells on an industrial scale. Successful particle detectors have been made by several workers, among them Kalbitzer (1967) and Meyer (1968).

who implanted at relatively low energies and annealed at temperatures of only 300-400 °C. Meyer reported energy resolution of 16.7 keV for 5.0 MeV alpha particles. Ion implanted position sensitive detectors have been made by Owen et al (1968) and Laegsgaard et al (1968). Position resolution has been reported to be as good as 0.2 mm in a detector 8 cm long.

Work has also been done on more elaborate devices. For example the fabrication of bipolar transistors entirely by implantation (Kerr and Large, 1968) utilizes the precise control over penetration depth. High frequency operation necessary in solid state microwave oscillators requires uniform, abrupt junctions. The manufacture of ion implanted IMPATT (Impact Avalanche Transit Time) diodes which can generate 1.5 watts at 10 GHz has been reported by Mankarious et al (1967).

A group at Ion Physics Corporation (Kellett et al, 1966) has reported the production of both n-channel and p-channel FET's. Usable frequencies for these devices is reported to extend into the 5 GHz region. Bipolar transistors fabricated by the same group, using ion implantation, showed typical transistor characteristics, but had high leakage, poor contacts, and high collector saturation resistance.

One of the most significant advantages of ion implantation has been shown in the fabrication of MOS FET's. Interelectrode parasitic capacitance has been significantly reduced in a method described by Bower and Dill (1966), in which the metal gate electrode is used as a mask to provide automatic registration of the electrode structure. The major part of the drain and source electrodes are put in by diffusion. Then after the gate electrode is deposited, implantation is used to provide better registration of electrodes.

Presently interest is still increasing in the implantation technique.

As this interest continues to grow, and more investigators work with the method, many new devices and techniques can be expected in the future. Also many researchers are becoming interested in implantation into insulators, or wide band gap materials.

PREPARATION OF CRYSTALS

Up to this point discussion has been only of results reported by other investigators. In this section a short description will be given of the procedures used in preparing the samples for implantation. In the following section, a complete description of the implantation apparatus will be given. The section following that will outline the testing procedure used to determine the characteristics of the implanted devices, and a summary will then be given of the results of those tests.

The substrate crystals to be implanted were provided by Motorola, and were of three resistivities:

12--15	ohm-cm n-type
60--100	ohm-cm n-type
6.5--7.0	ohm-cm p-type

All were 0.030 cm thick, polished on one side with the $\langle 111 \rangle$ direction within 3° of the normal to the crystal surface.

Each two-inch diameter wafer was scribed and broken into rectangular wafers 0.70 inches wide and 1.40 inches long. Extreme care was taken in this and all subsequent operations to avoid touching the wafers by hand. All handling was done by plastic or metal tongs. The crystals were then cleaned in ethanol, distilled water and warm concentrated nitric acid. For etching, the crystals were mounted in simple holders fashioned from tygon tubing. Etching was done in a 90% solution of CP4A at room temperature.

CP4A is a mixture of:

2 volumes	concentrated nitric acid
1 volume	glacial acetic acid
1 volume	40% hydrofluoric acid.

Typical time in the 90% etch was thirty seconds. To avoid exposing the crystal surfaces to air, large volumes of distilled water were used to

flush the etched wafers. Only after the solution had been diluted to less than one per cent, were the wafers transferred to pure water and rinsed. To give a smoother surface, transfer was then made to a 75-80% solution of CP4A where the crystals were left immersed for up to three minutes. After final flushing, rinsing and drying, the wafers were mounted for implantation.

The mount used for the implantation of these crystals is shown in Plate IV. The body was machined from lucite one-half inch in thickness. Stainless steel sheet 0.010" thick served as a mask to define the areas of the silicon wafers to be exposed to the beams. The silicon slices were held securely in place by stainless steel clamps which gripped the edges of the crystals. These clamps served as the electrical connections to the silicon and thus provided a means of monitoring the beam current during implantation.

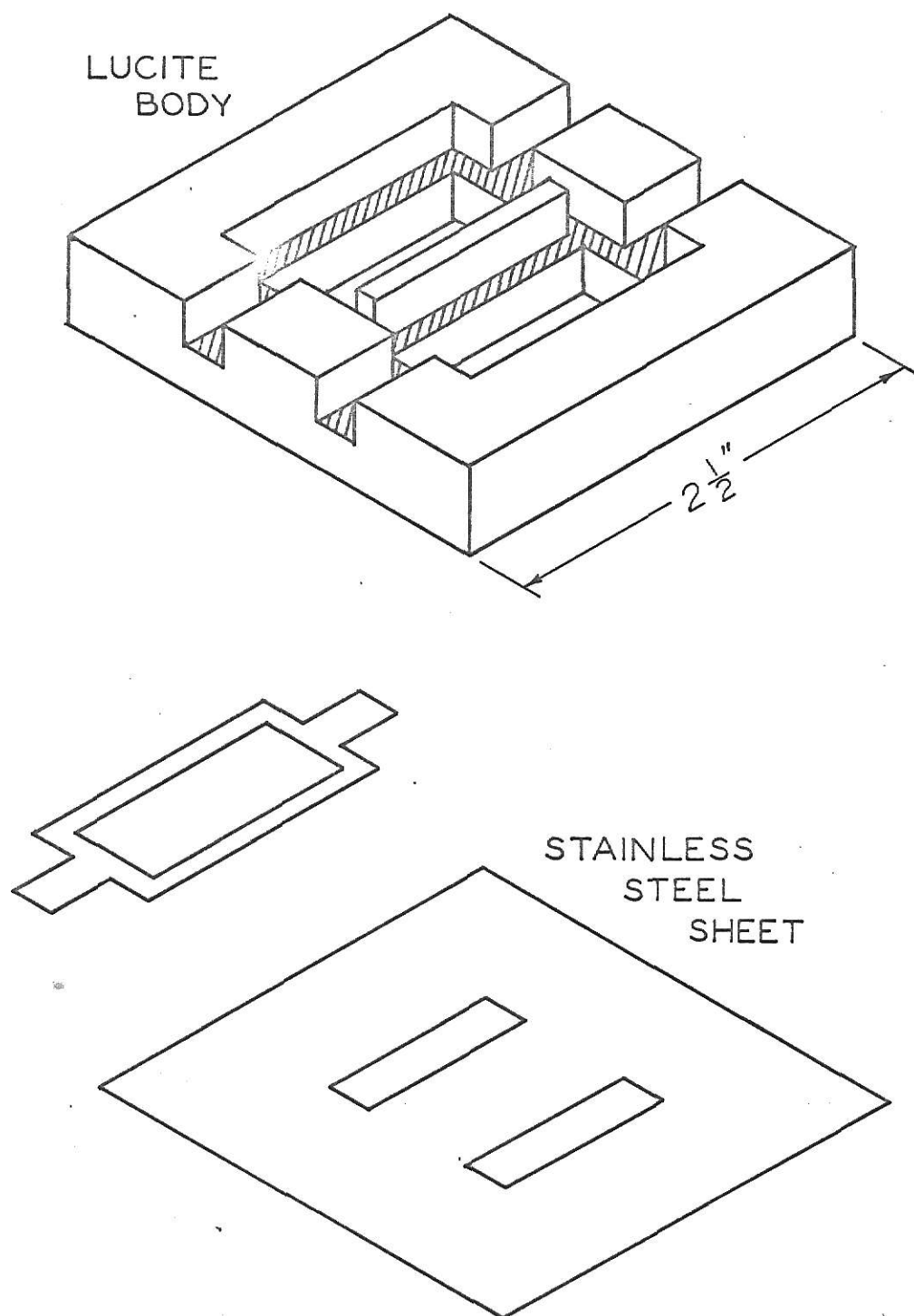
This lucite holder was then attached to the end of a sliding brass rod which allowed the holder to be moved and rotated from outside the vacuum chamber. Four electrical feed-throughs were wired--one to each crystal and one to each of the front and rear metal masks.

Typically during implantation, the holder could be oriented so that first a phosphorus beam was allowed to impinge upon the rear contact area. This area, whose cross section was one-quarter by one inch, would be doped to a level of about 10^{16} ions/cm². Then the holder would be rotated and the two contact regions of each of the two wafers' front surfaces were implanted with boron ions to a level of about 10^{16} ions/cm². These contact regions were about one-sixteenth by three thirty-seconds of an inch in area and were positioned approximately one inch apart on the front surface. A second sliding brass rod could then be used to remove one of the masks, exposing a one-quarter by one inch rectangular aperture through which boron

EXPLANATION OF PLATE IV

Shown in the upper figure is the machined lucite body in which the crystals were mounted for implantation. The metal sheets shown below were used to clamp the crystals in place and to serve as masks to define the area to be implanted.

PLATE IV



ions were implanted to a dose of about 10^{13} ions/cm², thus forming the "active" region. Ion doses in this active region could be varied to provide the desired resistance between the two front contacts and also to adjust the depth of the p-n junction. If the contact regions were to be formed by evaporation of pure aluminum onto the crystal surfaces, four, rather than two, wafers could be mounted simultaneously as implantation would be used to define only the active area between the two front contacts.

IMPLANTATION APPARATUS

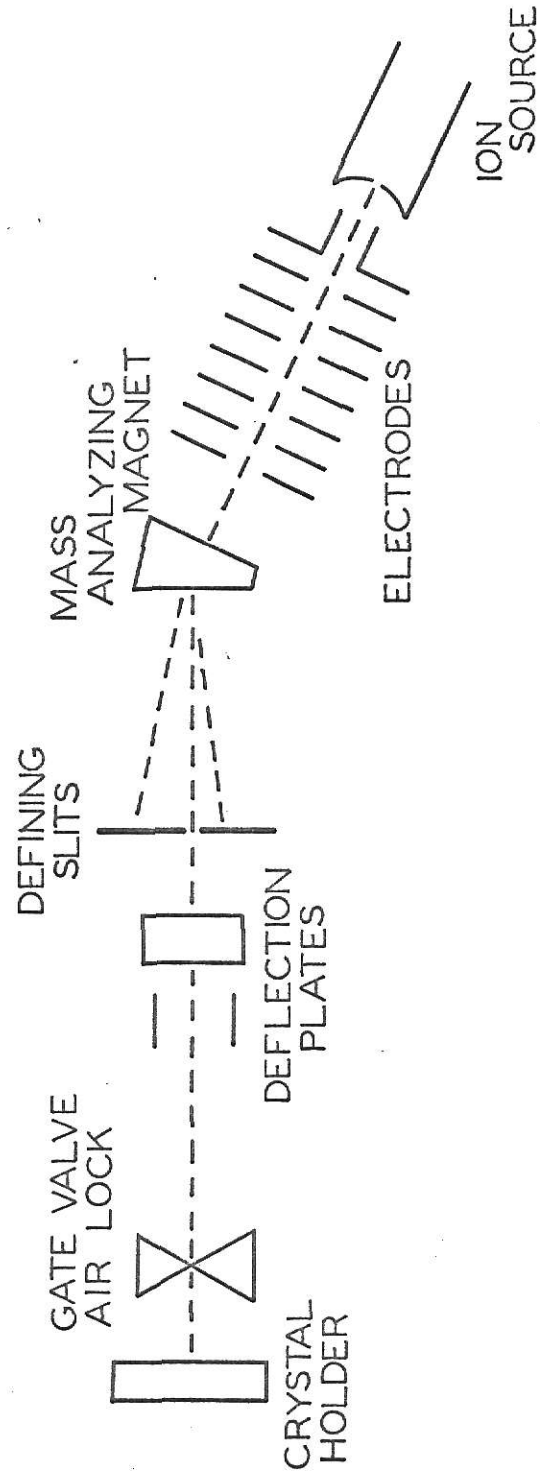
An overall schematic of the ion accelerator and implantation apparatus is shown in Plate V. The Physicon model 910 ion source, which is of the oscillating electron type, has proven to be quite versatile and does an adequate job of producing beams of singly charged boron and phosphorus ions as needed for this project. The few difficulties encountered in using this source were apparently caused entirely by the selection of gases used. Phosphorus pentafluoride served as the source of ^{31}P ions and boron trifluoride provided ^{11}B ions. Both these gases were highly corrosive and their use necessitated frequent cleaning of all parts with which they came into contact. To minimize gas flow regulation problems, a two-liter flask was evacuated, then filled to nearly atmospheric pressure with the desired gas from the high pressure cylinders in which they were shipped. A mechanical needle valve then gave sufficient control over the gas flow from flask to source. It was found to be extremely important that there was no contamination in the flask. Any residue such as water vapor or a bit of air, would drastically affect the performance of the ion source and lead directly to unstable, low values of ion current onto the target. The system of lines, valves and containers used to flush out the gas handling system is shown in Plate VI.

Accelerating voltage for the ions was provided by a Spellman power supply whose output was variable up to 150 kV. A series string of fifteen 100 Megohm resistors was connected between the high voltage Faraday cage and ground. This string could be tapped at any junction of adjacent resistors and the appropriate voltages could thus be applied to the accelerating electrodes. The lens system was thus formed from the seven individual aluminum electrodes

EXPLANATION OF PLATE V

This schematic shows the arrangement of equipment needed for a typical implantation system.

PLATE V

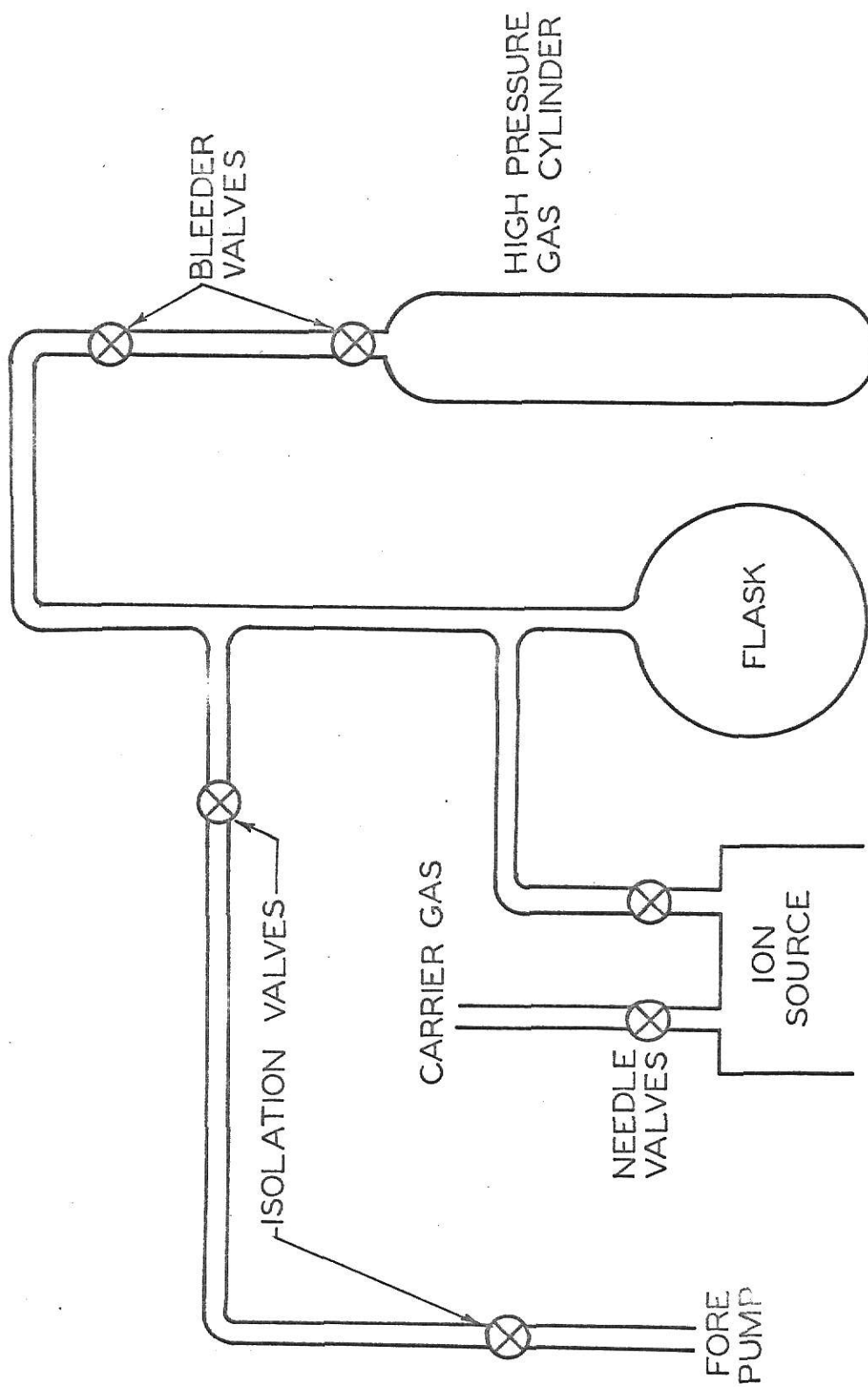


TYPICAL ION IMPLANTATION SYSTEM

EXPLANATION OF PLATE VI

Detail of the gas handling system used to provide boron trifluoride or phosphorus pentafluoride for the ion source.

PLATE VI



and lucite insulators.

Within the high voltage Faraday cage, a variable 0--20 kV negative power supply provided a selectable voltage to the first of these electrodes, the extractor, which was of greatest importance in the beam focusing. Mounted in an equipment rack within the Faraday cage were power supplies which provided current for the filament, discharge arc and source magnet. Gas cylinders and reservoir flasks with precision needle valves were also mounted within this equipment rack. Remote control for all these supplies and valves was provided by nylon control rods extending from the control shafts through a grounded protective cage which completely surrounded the high voltage terminal. The only access gate to the high voltage area was interlocked with the high voltage supply to provide personnel protection.

Because of the large amount of heat generated by the operating ion source, it was necessary to employ a heat exchanger. Transformer oil (to provide high voltage isolation) was pumped through cooling coils in the body of the source. This circulating oil was in turn cooled by cold tap water in a simple heat exchanger.

Mass analysis of the accelerated beam was accomplished by deflection at a 25° angle by an electromagnet and well-regulated power supply system made by High Voltage Engineering Corporation. At distances of approximately 30 cm and 52 cm behind the magnet were ports for mounting collimating slits of desired shape and size. The intention was to use apertures as large as possible to allow maximum beam intensity, yet small enough that satisfactory beam purity was provided by eliminating essentially all unwanted ion species. A simplified explanation of this mass separation technique might proceed as follows:

The force on a charged particle moving through a transverse magnetic field is given by:

$$F = Bqv$$

where B = magnetic field strength

q = charge on particle

v = velocity of particle

The result is a circular trajectory, with a radius given by:

$$r = \frac{mv}{Bq} = \frac{\sqrt{2mE}}{qB}$$

m = mass of particle

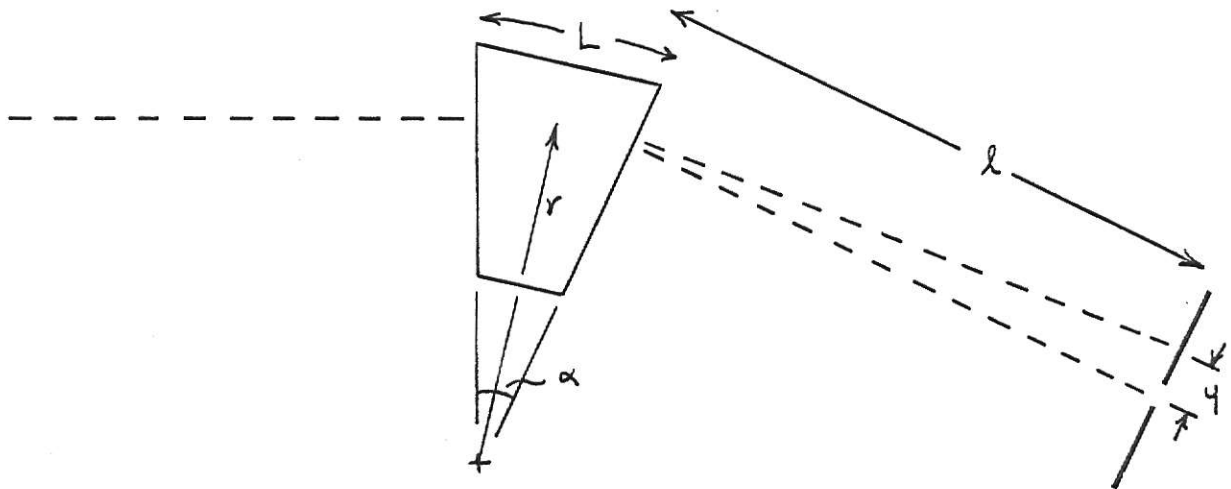
E = energy of particle

Since for the usual type analyzer system, the radius is fixed by geometry, we must have:

$$mE = kB^2$$

where k is a constant of the system

To get an estimate of the separation of nearly equal masses at the defining slit, consider the usual sector type magnet separation system.



As a first approximation, assume that the particle path (L) through the magnet is nearly equal for adjacent masses.

Then;

$$\alpha = \frac{L}{r} = \frac{LBq}{\sqrt{2mE}}$$

So the separation of nearly equal masses at the slit is

$$y = \Delta\alpha l = \frac{\alpha l}{2m} \Delta m$$

The two collimating slits following the magnet thus served to define the size of the ion beam. When scanning through the various accelerated ion masses, it was found that the carbon peak (^{12}C) was usually of comparable size to the boron beam. Considerable amounts of $^{14}\text{N}_2$ and $^{16}\text{O}_2$ would often be present to give trouble in selecting the ^{31}P ions. By using the mass separation formula given earlier, the separation of the mass 31 and 32 beams can be calculated to be 0.16 inch at the second slit. Apertures as large as one-eighth inch diameter could then be used to give adequate separation of these adjacent peaks. After choosing these slits to obtain adequate mass separation, there was difficulty in obtaining a spot size larger than one quarter inch diameter at the crystal. Because of the small size and the presumed non-uniform current density over this area, two pairs of electrostatic deflection plates were located just behind the last collimating aperture. To facilitate the highest uniformity in doping over the entire surface of the exposed crystal, the beam was scanned linearly over an area which extended well beyond the exposed crystal. Triangular waveforms of variable voltage were applied to horizontal and vertical pairs of deflection plates. A frequency of 20 Hz was used for vertical motion of the beam, and a non-phased 400 Hz signal provided horizontal motion.

The crystal holder itself was mounted about 62 inches behind the last collimator and 35 inches behind the last deflection plate. A gate valve near the crystal mount gave an air lock capability, allowing the removal and mounting of crystals by venting only a small portion of the vacuum chamber.

Following implantation, the crystals were ready for either annealing or contact formation.

TEST PROCEDURE

After being implanted, the crystals were prepared for electrical testing. For most of the tests, an aluminum film was evaporated onto the crystal surface to facilitate the formation of a contact to the implanted silicon. High purity aluminum wire was used as the source of contact material. A short length (about one inch) of this wire was placed inside the coils of a tungsten filament which was then heated in vacuum by the passage of a current. When melted, the aluminum would alloy to the tungsten. Further heating caused this alloyed aluminum to evaporate off onto the exposed areas of the crystals. This contact formation was accomplished inside a Veece model 776 evaporator at a usual pressure of less than 3×10^{-6} Torr.

Well aligned stainless steel masks (0.010" thickness) were used to expose only that portion of the crystal onto which aluminum was to be evaporated. No special cleaning procedures were used on the surfaces between the implanting and evaporating steps. Only a few of the contacts formed in this manner failed to exhibit ohmic characteristics, but perhaps the failure of those few could be attributed to the presence of some surface contamination. No definite attempt was made to determine the thickness of the evaporated aluminum film, although a crude estimate could be made by observing the opacity of the film deposited on a glass microscope slide placed adjacent to the crystals during evaporation. The method led to an estimated film thickness of about 1000 Å.

Annealing of the implanted silicon chips was done inside a three-quarter inch I. D. quartz tube which in turn was inserted into a cylindrical oven. A flow of gas such as argon or nitrogen could be circulated through the quartz tube, or alternatively, a vacuum (pressure of about 2×10^{-6} Torr) could be

maintained during the annealing process. Annealing temperatures were monitored by means of an iron-constantan thermocouple. The reference junction was in an ice bath and thermoelectric voltages were measured with an electrometer. The temperature calibration used for the iron-constantan thermocouple was $17.98\text{ }^{\circ}\text{C/mV}$.

For the electrical tests performed on the completed diode structures, the crystals were mounted in holders made of Vespel. Vespel is a trade name for a special machinable plastic made by Du Pont. The two halves of this plastic unit clamped over the silicon wafers and held the spring-loaded beryllium-copper probes securely in place at the proper position on the crystal surfaces. In nearly all tests, this holder was mounted inside a chamber pumped down to a pressure of a few microns of Hg by a mechanical pump. Eight electrical feed-throughs were provided to connect to the contact wires. Two probes positioned about one mm apart made contact on each of the two front contact areas. This arrangement allowed the determination of the resistance associated with the contacts only, independent of bulk semiconductor effects. A total of four probes made contact to the rear surface of the crystal. Having these eight separate contacts permitted the measurement of contact resistance, active area resistance (effectively sheet resistance) and current-voltage characteristics of the diode structure. With the associated metal shields in position, the same holder could be used for particle detection if the crystal was used in the particle detector mode.

A few difficulties were observed in the process of preparing and implanting the silicon crystals. Some of the more common problems will be mentioned in the following. A few of the crystals were slightly damaged in the etch process. Occasionally pits would form on the silicon surface

where the CPH_4 etchant solution attacked more vigorously. It was empirically noted that there seemed to be an optimum concentration for the CPH_4 at which the best polish was put on the surface. At room temperature, this seemed to be about a 75% solution. If the etch process proceeded either too fast or too slowly, irregularities were more likely to form on the surface. Several times trouble was noted whenever a new mixture of CPH_4 was used. The three acids would be mixed well by agitation, but it seemed to be necessary to allow the mixture to stand for some time before use. Failure to allow the CPH_4 to stand for at least a half-hour seemed to result invariably in a discoloration of the silicon surface. A smooth flat surface on the wafer to be implanted was highly desirable as the concentration of implanted impurities could be expected to follow very closely the topography of the surface. For optimum detector performance, especially under reverse bias, the p-n junction should be as flat and as uniform as possible.

The use of two separate slits behind the mass analyzing magnet was not a necessity for separating the different ion species. However the use of these two apertures, rather than only one, defined a single trajectory through the magnet which the ions could follow. Also it limits the divergence of the ions and thus permits a more uniform scan on the crystal. The use of the two slits became especially important since our system was run with no defining aperture ahead of the analyzing magnet. In the usual tune-up procedure, the desired ion beam would be maximized through the first aperture, then source parameters and deflection magnet would be varied until a maximum of that beam was then passing through the second aperture. This simple procedure would assure that a maximum beam of highest purity would strike the mounted crystal and that the scanning pattern could be centered.

In the mass analysis, occasional difficulty would be encountered in

positively identifying which mass ion was passing through the slit system. Eventually a technique was worked out which gave a high certainty of results. A voltmeter connected to a hall probe sensor in the mass analyzing magnet allowed the operator to accurately determine the mass ratios of all separated and detected species. Comparison of the relative magnitudes of these various ion currents could then identify these masses. In the case of boron, which has two predominant isotopes, this method was quite reliable. About 80% of natural boron has a mass of eleven amu, while the other 20% has a mass of ten amu. The ratio of the boron ion beams at masses eleven and ten would be in the same ratio as the natural abundances of these two isotopes, 4:1. Mass twelve carbon ions and mass nineteen fluorine ions would always be present also to serve as calibration points. Positive identification of the ^{31}P ions was somewhat more difficult, because of the comparable magnitudes of the $^{14}\text{N}_2$ and $^{16}\text{O}_2$ beams. The only reliable technique found was that of scanning through all masses with and without phosphorus in the ion source. Only the magnitude of the phosphorus ion beam would change drastically in this process.

The current measured on the silicon wafer during ion bombardment would be in error by an amount equal to the secondary electron current. Comparisons of measurements made on a shielded Faraday cup, as well as noting the effects of applying bias to the shield in front of the crystal surfaces indicated that the secondary electron yield for 60 keV boron ions on silicon would be about 1.2 (i.e. 1.2 ejected electrons for each incident ion). Because of the relatively large crystal area exposed to the beam, it was considered impractical to attempt to totally inhibit all secondary electron emission. Instead, the shield immediately in front of the crystal surface was run at ground potential, and the value of current as measured by the electrometer

was divided by two. This procedure was believed to give an accuracy of about 30%, and in view of previous measurements could be expected to be in error by less than a factor of two.

A persistent problem was that of annoyingly low beam currents. Generally the maximum obtainable boron beam was about 100 nano amps. After the scanning system spread this amount evenly over the crystal mask, only about one-twentieth that amount would strike the crystal surface, so typical operating ion beams were five nano amps on each wafer.

RESULTS

A total of fifty samples for implantation study were cleaved to 0.7 by 1.4 inch rectangular size from the silicon wafers supplied by the Motorola Semiconductor Product Division. These were run through various stages of preparation and testing. After having been cleaved, each crystal was run through the steps of cleaning, etching, implanting, annealing, contact formation and testing. After initial testing, some wafers were then run again through some of those steps as well as additional surface treatments.

Primary concern during the entire program was to produce devices showing acceptable diode characteristics. Then later, those with diode properties were to be tested as particle detectors. However very early in the testing procedure it was observed that there was difficulty in producing ohmic contacts at the point where the metal conductors made contact with the silicon. For some reason not understood at present, contacts made either by using a heavy (high dose) implantation, or by deposition of an aluminum film never did form perfectly ohmic contacts with the silicon. Perhaps a different form of surface treatment from what was used could have modified the surface states of the silicon sufficiently that ohmic contacts could have been formed. At present there is no assurance that the wafers would have been useful detectors if only the contacts were ohmic, but at least they could have been expected to show diode characteristics at the p-n junction formed by the implanted impurities.

In the following, a discussion will be given of the results of tests performed on the crystals. Considerable time was spent on those devices having implanted contact areas in investigating the resistive or diode properties of the junction between the metal and the silicon.

If only pressure contacts were used, the diode properties of the metal-semiconductor interface would completely obscure any diode qualities which may have existed at the junction within the bulk material. The next step was to fuse or "wipe" adjacent contacts by momentarily passing relatively large currents through them. It was found that a-c worked best for this and that a current of nearly 90 mA was usually needed to produce contacts which no longer showed diode properties. Even in those cases when the current between adjacent contacts was nearly proportional to the applied voltage, the resistance associated with the contacts remained so high (about 15 K ohms) that it could effectively mask the resistance across the front active area.

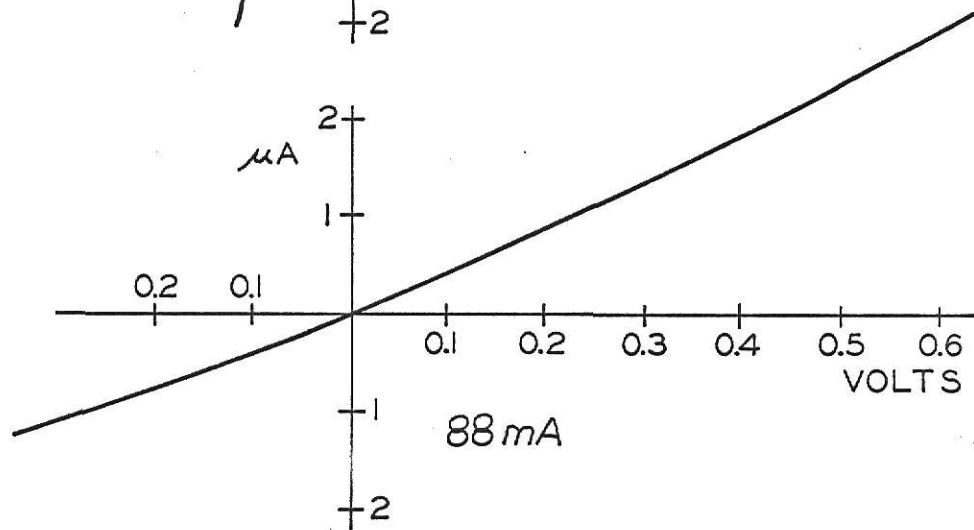
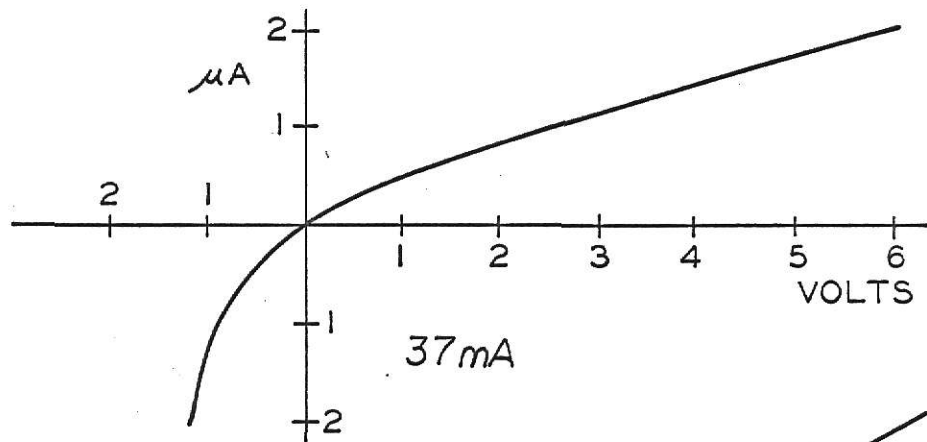
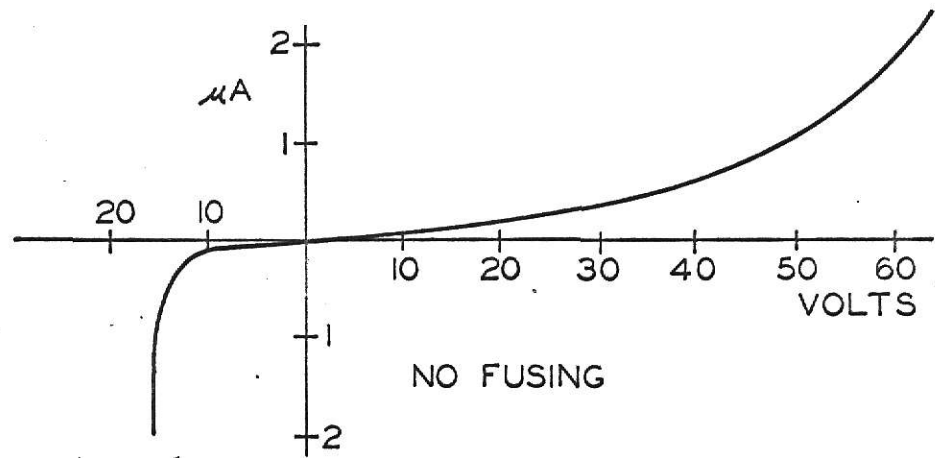
The effect of various values of fusing current on the forward-reverse characteristics of crystal #4 is shown in Plate VII. Such behavior was fairly typical of several of the crystals treated in similar manner. It is easily seen that all apparent diode properties disappeared when higher currents were used. Current-voltage measurements from implanted region to bulk indicated that what should have been a p-n junction was perfectly ohmic in both directions! If indeed the junction had been present within the silicon sample, there should have been leakage currents of less than one microamp even with several volts reverse bias. The observed behavior led to speculation that perhaps the implanted contacts on the front surface were extending beyond the implanted active region and that the current was thus bypassing the implanted junction. Still no explanation could be given as to why no junction could be seen between the implanted contacts and the n type bulk material.

Since the difficulty with such contacts seemed to occur just at the metal-semiconductor interface, it was decided to try evaporating metal onto the implanted region. It was hoped that the much larger area of contact

EXPLANATION OF PLATE VII

Graphs showing the effect of fusing current on the electrical properties between front and rear contacts on crystal # 4. The first graph shows the characteristics found with no fusing current--pressure contacts only. The second was taken after a fusing current of 37 mA was used between adjacent contacts. The third, showing nearly ohmic behavior occurred after a fusing current of 88 mA.

PLATE VII



would permit a low resistance ohmic contact with the doped semiconductor material. Also the spring-loaded contact probes could be expected to make an excellent contact with the evaporated metal. Aluminum was chosen for it could be evaporated easily and was available in a high purity (0.99999) form. The evaporating procedure has been described in an earlier section, so only the test results will be mentioned here. With the aluminum films now serving as the contact areas, it was no longer necessary to attempt fusing of adjacent contact wires, for resistances from one point to another on the same film were of the order of one ohm.

To facilitate faster checking of diode properties, the complete series of current-voltage readings was omitted and resistances between various contacts were checked with a Simpson VOM model 260. Some error was expected from this limited test procedure, but this method should still have given an indication of contact resistance, impedance across front active area, and would indicate if the junction formed by the implanted ions was ohmic or showed some diode properties.

A complete description of the results of tests on all the devices will not be given. Instead, detailed descriptions are given for only a few properties of some of the implanted crystals. Those chosen will represent typical behavior of specially interesting results. A non-detailed summary of all crystals tested is given in Table I.

On the first two crystals with evaporated aluminum contacts, only the front contacts were put on the first time. Measurements made on those were sufficiently promising to justify an expanded series of tests on more such contacts. Crystal #114 was the first to have a complete set of evaporated contacts. Tests on it indicated some unwanted polarity effects in the measured resistances on the contacts, as well as perfectly ohmic behavior

EXPLANATION OF TABLE I

Explanation of column headings:

crystal #	refers to the identification number assigned to that crystal.
doping level	gives the number of ions implanted per square centimeter onto the exposed crystal surface. This number was based on a correction of the measured charge deposited on the silicon during implantation. The number following the hyphen gives the energy of the incident ions in keV.
anneal temperature	the letter indicates the environment in which the crystals were heated. "v" indicates low pressure (about 2×10^{-6} Torr). "a" indicates an inert gas atmosphere. The maximum temperature to which the implanted wafers were raised is indicated also, in units of degrees centigrade.
contact resistance	"i" indicates contact areas put in by a high dose implantation (about 10^{16} ions/cm ²) "e" indicates that the contacts were made by evaporation of high purity aluminum onto the specified areas. The numbers give typical values for measured resistances between adjacent contacts. In the case of implanted contact areas, this value was measured after contact fusing.
diode properties	This indicates the resistance measured in both directions from front contacts to the rear contacts. If no diode characteristics were seen at all, it is designated "ohmic", followed by the approximate value of this measured resistance. For units which showed diode properties, two methods have been used: two resistances indicate respectively the measured forward and reverse values of resistance. If the implanted crystal was indeed a reasonably good diode, then the words abrupt or soft to indicate an abrupt or slow reverse breakdown, are followed by numbers which indicate the approximate voltage at which breakdown occurred.

TABLE I

SUMMARY OF RESULTS ON IMPLANTED WAFERS

crystal #	type	doping level	anneal temp	contact res	diode properties
1	n	1.0-60	a-490 a-615	i-20K	140K-330K 20K-80K
2	n	1.0-60	a-490 a-615	i-20K 1.1K	100K-2Meg 1.7K-30K
3	70n	0.72-50	a-480 a-550	i-50K	60Meg-1Meg broken
4	14n	1.7-50	a-480 a-550	i-11K i-100K	13Meg-2Meg ohmic-13K
5	14n			e	15-100 ohms
6	70n			e-1.0K	33K-5Meg
7	70n	surface damaged in etch.			
8	70n	0.3-60	v-460	e	
9	70n	0.2-25 0.1-60	a-450 v-550	i-3.0K 12K	ohmic-30K ohmic-20K
10	70n			e	2.8K-4.0K
11	70n	surface damaged in etch.			
12	14n	0.3-60	v-460	e-80 ohm	ohmic-0.5K
13	14n	114-60	v-530	electron micrographs	
14	14n	0.2-25 0.1-60 0.2-60	a-450 a-460	i-30K e-1.4	ohmic-14K 200K-50K
15	6p	0.3-60	v-320	e-4.0	10K-1.1Meg
16	6p	0.3-60		e	broken
17	6p	0.4-60		e	
18	6p	0.4-60	v-320	e-0.2	650K-80K
19	6p	surface damaged in etch			
20	14n	surface damaged in etch			
21	14n	0.3-60 8.0-60	v-320	e-20 e-5.0	abrupt-14 20K-12Meg
22	70n	0.3-60	v-320	e-0.3	ohmic-60 ohm 0.9K-3.6K

TABLE I (continued)

crystal #	type	doping level	anneal temp	contact res	diode properties
24	70n	10-60		e	10K-650K
25	70n	0.9-60 0.3-25	v-310	e-1.2	ohmic-100 ohm
26	70n	0.9-60 0.3-25	v-310 a-680	e-1.0 e-3.0K	ohmic-2.0K 20K-170K
27	70n	0.9-60 0.3-25 8.0-60	v-310 a-680	e 2.0 1.5K	abrupt-10 10K-800K 14K-100K
28	70n	0.9-60 0.3-25	v-360 a-680	e-2.0 3.0K	ohmic-300 30K-120K
29	14n	0.2-25 0.8-60	v-310	e	broken
30	14n	0.2-25 0.8-60	v-310	e-0.8	abrupt-10
31	14n	0.2-25 0.8-60	v-310	e-2.0	soft-6
32	14n	0.2-25 0.8-60	v-360	e-1.5	ohmic-50 ohms
33	6p	0.3-60 0.6-25	v-310	e	ohmic
34	6p	0.3-60 0.6-25	v-310	e	
35	6p	0.6-60 0.6-25	v-310	e-1.0 e-1.0	180K-1.3Meg 2.0K-57K
36	6p	0.6-60 0.6-25	v-360	e-1.4	1.5Meg-100Meg 16K-400K
40	70n	10-60	v-445	e-1.2	1.5K-1.1K
41	14n	7.6-60	v-445	e-1.0	ohmic-150
42	14n	7.6-60	v-445	e-1.0	5.0K-100K
43	70n	16.8-60		e-1.0	broken
44	70n	16.8-60		e-0.8	ohmic-1.2K
45	14n	damaged in etch			

TABLE I (continued)

crystal #	type	doping level	anneal temp	contact res	diode properties
46	14n	damaged in etch			
47	70n	1.5-45	a-900	e-1.1	5.5K-2.1K
48	70n	1.5-45	a-900	e-1.2	8.3K-2.8K
49	70n	1.0-45	a-900	e-1.2	ohmic-7.5K
50	70n	1.0-45	a-900	e-1.4	4.5K-3.0K

from front to back across what should have been an implanted junction. Some extra care had been taken when making the metal mask through which aluminum was evaporated onto the faces of the crystals to ensure that the evaporated aluminum indeed was positioned on the implanted region and did not extend onto the unimplanted bulk silicon.

A test chip (crystal #6) was etched, but was neither implanted nor annealed before deposition of contacts. Tests made on it showed some very definite diode behavior (Fig. 5). This effect was an absolute indication that extreme care would have to be exercised to insure that the characteristics of any metal-semiconductor interface would not be mistaken for the implanted junction within the bulk.

Some of the p type substrates were implanted with phosphorus ions in an attempt to see if a definite junction could be seen in them. All those tested were either perfectly ohmic or, if they showed some polarity, had leakage currents far too large ($2\mu\text{A}$ at 0.1 V) to permit use as diodes.

Finally one of the 12--15 ohm-cm n type wafers (#21) showed some characteristics which were beginning to look reasonable. The active area on this sample was implanted at a level of only about 4×10^{12} ions/cm². First tests on this crystal were run immediately after contacts were laid on, and before any annealing. Forward-reverse resistances as measured by the VOM were 15 k ohms and 2 Megohms. I-V characteristics showed a soft reverse breakdown at about 6 volts. After annealing at 320 °C, further tests were run. A sharper breakdown was observed then, and at 11 rather than 6 volts. I-V curves for both before and after annealing are shown in Fig. 6.

Crystal #22 was treated identically to #21, except that it was annealed before deposition of contacts. It showed a very acceptable 16-20 k ohms across the front resistive region, but only 60 ohms for both polarities from

EXPLANATION OF PLATE VIII

Figure 5 shows data taken from an unimplanted, unannealed wafer (crystal # 6) on which aluminum contacts had been evaporated immediately after etching.

Figure 6 was made from data taken on crystal # 2] before and after annealing, showing the formation of an apparently good diode.

PLATE VIII

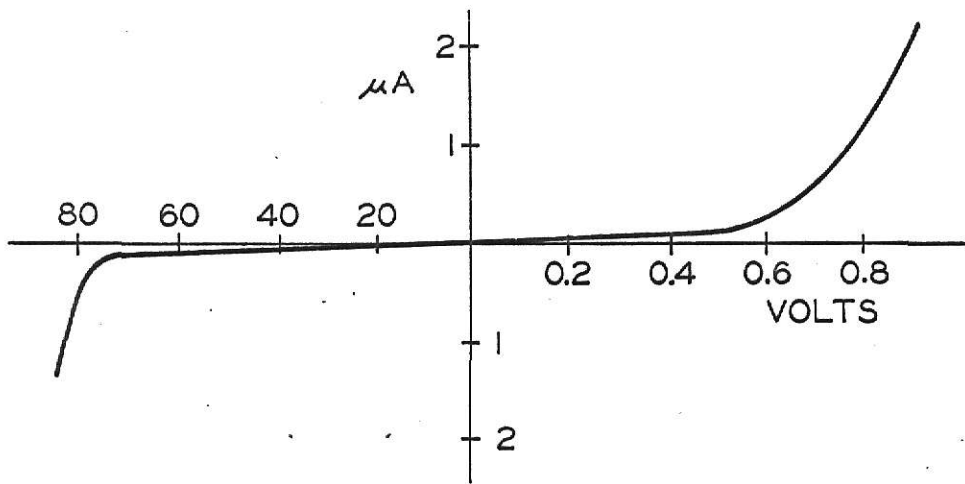


FIG. 5

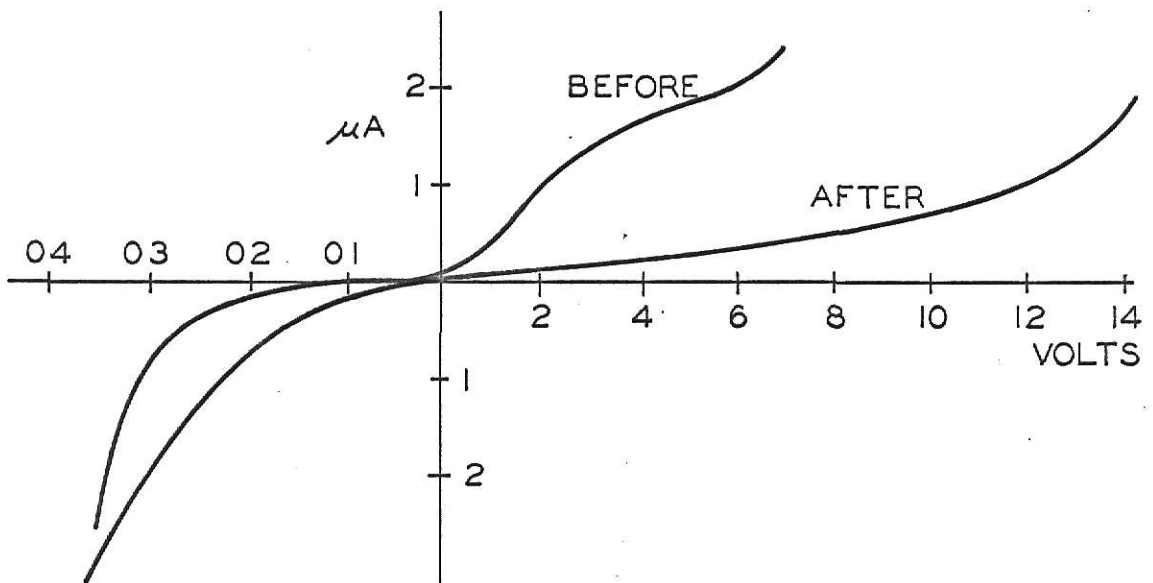


FIG. 6

either contact on the front to the rear contact area.

Since crystal #21 showed some promise by having acceptable diode properties, numbers 25-32 were prepared in a similar manner. Numbers 25-28 were doped with ^{11}B ions to a level of 9×10^{12} ions/cm² at 60 keV and 3×10^{12} at 25 keV. Crystals 29-33 were similarly doped to levels of 2×10^{12} at 25 keV and 8×10^{12} at 60 keV. Numbers 28 and 32 were annealed at 360 °C before contacts were put on. Both were perfectly ohmic in both directions in tests made between front and rear contacts.

Contacts were put onto the other wafers before the annealing stage. Number 31 showed some slight diode properties on the VOM, but drew nearly two microamps with a voltage drop of only 50 mV reverse bias. The behavior of #27 was very similar. Similar behavior was noticed for #30 with reverse breakdown occurring at 10 v. Numbers 25 and 26 again showed ohmic properties between front and rear contacts.

The next step was to test some of those four diodes as particle detectors. An ^{241}Am source was used to provide 5.48 MeV alpha particles. Pulses from these detectors were run into an ADC, then into a multichannel analyzer. Analysis of the MCA could give some indication of the noise and resolution associated with the detectors.

A major problem was observed when the completed devices were used as detectors; this was that the counting rate of pulses reaching the analyzer was too low to be very useful. Most importantly, the count rate was much lower than was to be expected from the geometry used and the emission rate of the calibrated alpha source. It was noted that the count rate was highly dependent upon the position of the alpha source with respect to the detector, so it was assumed that the alpha emission was merely anisotropic. Further deception was provided when a new commercial surface barrier detector also

indicated a lower than expected count rate. Later tests on this same alpha source established that the emission was indeed near normal and much higher than had previously been observed.

Verification of the fact that the alpha source was calibrated correctly meant that only a portion of the active area on the crystal surface was responsive to particles. Later tests performed by masking portions of that area then established that the only responsive region was either the metal film contacts, or the active area immediately adjacent.

In a test separate from the electrical ones described, the electron microscope was used to look for surface damage of the silicon caused by a high-dose implantation. A thin platinum carbon film was evaporated at about a 45° angle onto the surface of wafer #13. A very dilute mixture of CPLA was used to float the film off the silicon surface onto a copper mesh which was subsequently positioned in the electron beam within the microscope. The preparation of this crystal and the use of the microscope was directed by Dr. Derek Stirland.

Figures 7-10 show photos made from four regions of the silicon surface. No large scale damage is visible in the Fig. 7, made from an unimplanted region. Light damage is seen in Figs. 8 and 9, but the relatively large diameter (0.21μ) spots are almost certainly due to causes other than implantation, probably damage introduced during etching. An entirely different topography is shown in Fig. 10. This region showed massive damage, at least some of which may have been due to implantation. This work was not pursued further, as the study of damage effects was not a part of this program.

EXPLANATION OF PLATE IX

Transmission electron micrographs of platinum carbon replicas taken from the surface of silicon wafer # 13. (magnification 38,000)

Figure 7. Electron micrograph from unimplanted region.

Figure 8. From the implanted region of the silicon. Features shown are probably due to pits formed during an etch process.

**THIS BOOK
CONTAINS
NUMEROUS
PICTURES THAT
ARE ATTACHED
TO DOCUMENTS
CROOKED.**

**THIS IS AS
RECEIVED FROM
CUSTOMER.**

PLATE IX

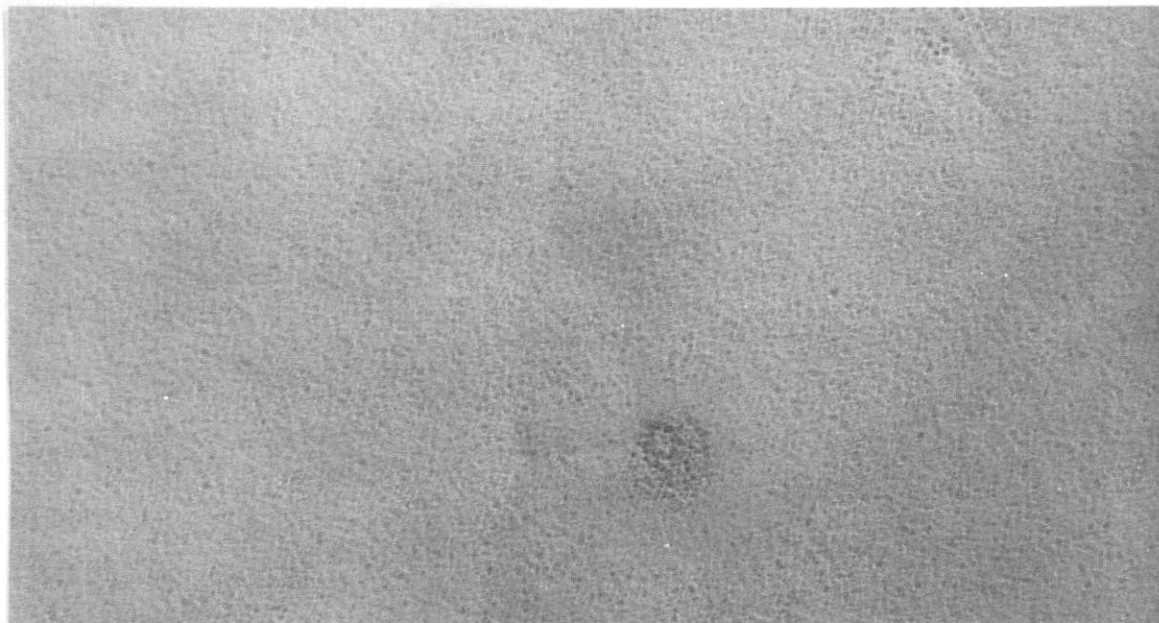


FIG 7

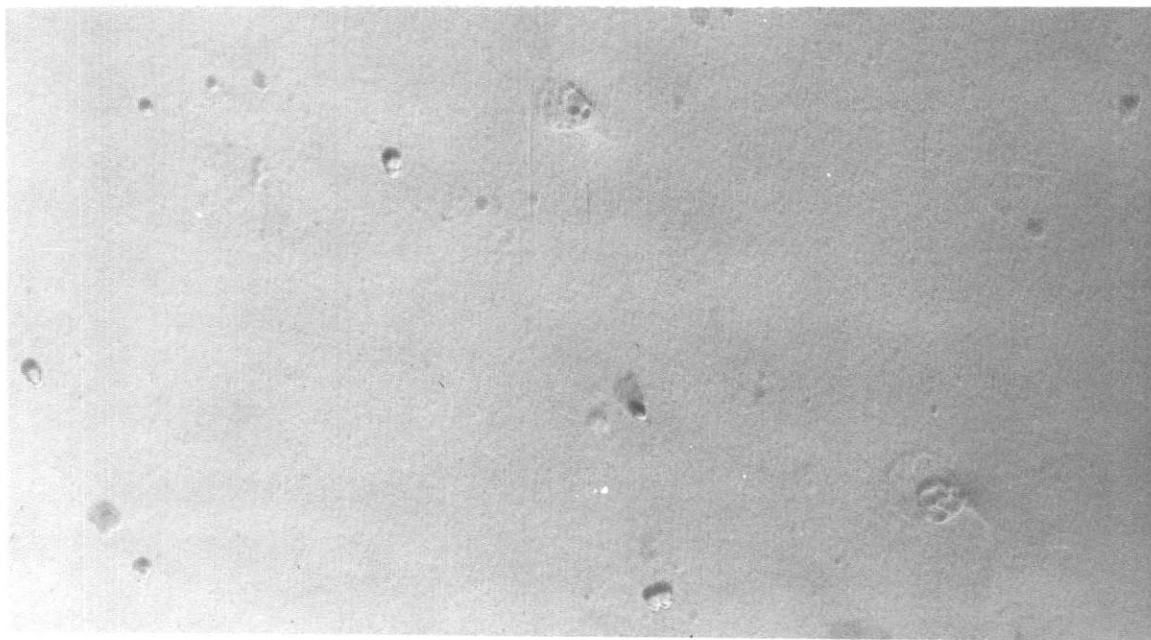


FIG 8

EXPLANATION OF PLATE X

Transmission electron micrographs of heavily implanted region of silicon made by using platinum carbon replicas with 38,000 magnification.

Figure 9. Damage regions due to etching.

Figure 10. Region showing extensive surface damage, perhaps due in part to the high dose phosphorus implantation.

PLATE X



FIG 9

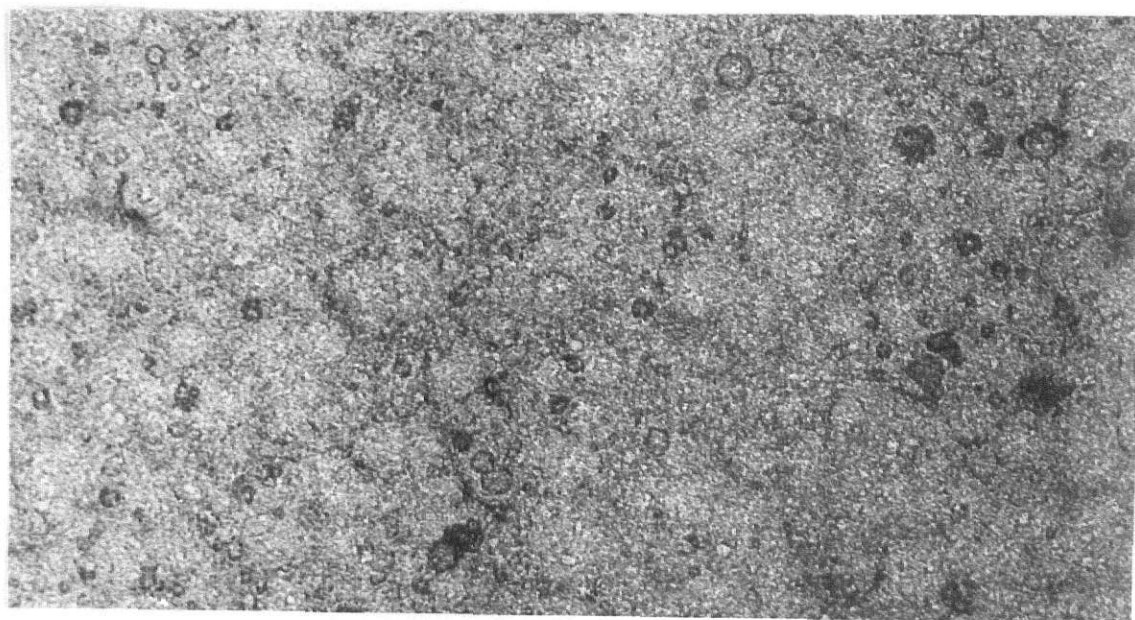


FIG 10

CONCLUSION

From the results of tests performed on the implanted samples, it seemed quite likely that all the diode effects which were seen resulted from contact effects at the metal-semiconductor interface. Also there was no assurance that pulses seen when the wafers were used as particle detectors arose from a junction within the bulk rather than from a surface barrier type diode formed by the deposited aluminum film. Apparently the p-n junction, which must exist due to the implanted impurities, was being by-passed or shunted in resistance measurements made between front and rear contact areas on the wafer. This would seem to be the only possible explanation as to why front-to-back measurements could indicate ohmic properties and no diode characteristics whatever.

The fact that different concentrations of implanted impurities made no detectable change in the properties is probably further proof that the true p-n junction was not being seen. Differing annealing temperatures, which could be expected to cause different fractions of the implanted atoms to be rendered electrically active, also produced no significant changes. One observed property which indicated the metal-semiconductor contacts as troublemakers was that annealing before contacts were made invariably resulted in ohmic properties on the crystal. The only samples which showed even traces of diode characteristics were some of those which had had contacts deposited before annealing. If the bulk p-n junction were being observed, the order of performance of those two steps would have been expected to make no difference. A change in surface properties of the silicon when the wafer was heated after deposition of metal could perhaps account for some of the diode properties seen.

Had the implanted active area been responsive to particles, the height of pulses from one end of the front region could be expected to be somewhat dependent upon the position at which that particle struck this area. No such variation in pulse height was seen.

In some work which was done concurrently with the research reported here, identical silicon wafers were implanted to a dose of 2×10^{14} ions/cm² with 60 keV boron ions. Those implanted crystals were subsequently sent back to the Motorola Semiconductor Products Division in Phoenix. There they were run through the steps normally used to fabricate high frequency bipolar transistors, with the implanted region serving as the base in the transistor structure. Device yield from the scribed wafers was reported to be about 15%, just slightly lower than usual for similar devices made entirely by diffusion. Frequency response on some of these transistors was reported to extend into the 5 GHz region. Reverse voltage breakdowns went as high as 40 volts.

The success of those devices should establish that the semiconductor material used as a substrate for implantation was not at fault. Perhaps that was not really true, as there has been some speculation that having such a large area (1.6 cm²) junction, lowers to near zero the probability of finding a successful junction. Even a very tiny "bad" region in the crystal could effectively short out the junction. Typical active areas on most common devices is a square 30 to 100 mils on a side. With them, the yield of good devices from a large wafer is almost never 100%. At least there is evidence that the boron implantation itself is not to blame for the failure of the diode. It is believed that instead the problem must lie somewhere in the steps of annealing, contact formation, or other treatment.

Probably the most encouraging sign from any of the tests on the crystals came when testing the photosensitivity on crystal #2. This was one of the

last tests performed on any of the implanted wafers and came after the evaporated aluminum contacts had been removed by NH_4OH . After a very light etch to remove a thin layer from the surface, contacts were fused onto the exposed heavily implanted regions. As had been noted before, ohmic contacts were very difficult to form, but on those that were ohmic, the photo-sensitivity was observed to extend over the entire implanted active region of the crystal surface, and was not limited to the contact areas. Even then the observed electrical diode behavior between front and rear was poor. When fusing the contacts, it was difficult to obtain reproducibility or to form ohmic contacts with less than about 20K ohms resistance.

If the junction did indeed exist within the bulk, it must be assumed that neither the implanted nor the evaporated contacts were "touching" the implanted active area. When attempts were made to fuse contacts onto the heavily implanted regions, it is possible that damage was introduced into the crystal which then destroyed the junction in the bulk. However there should have been no damage caused by the evaporated contacts, and some of them showed ohmic properties from front to rear.

It is thus quite obvious that some other method must be found to produce contacts before proper tests can be performed upon the implanted junctions. True behavior of regions within the bulk of the semiconductor will be difficult, if not impossible, to observe until reliable ohmic contacts are formed onto the surface.

ACKNOWLEDGMENT

The author wished to express his sincere thanks to Dr. James R. MacDonald for his initiation of this project and for his assistance throughout the program. Appreciation is also in order for the many others who offered very helpful suggestions. Financial support for the project was provided by an NDEA Fellowship and by the accelerator fund at Kansas State University.

REFERENCES

- Alvager, T. & N. J. Hansen
Rev. Sci. Instr. 33 567, (1962)
- Bethe, Hans A.
Ann. Physik 5 325, (1930)
- Bloch, T.
Ann. Physik 16 285, (1933)
- Bohr, N.
Phil. Mag. 25 10, (1913)
- Bower, R. W. & Dill, H. G.
Proc. Int. Meeting on Electron Devices, Washington Oct. 1966
- Bredov, M. M., V. A. Lepilin, I. B. Schestakov, & A. L. Shakh-Budagov
Sov. Phys. - Solid State 3 195, (1961)
- Crowder, B. L. & J. M. Fairfield
Trans. of Met. Society of AIME 245 469, (1969)
- Davies, J. A., J. Friesen, & J. D. McIntyre
Can. J. of Chem. 38 1526, (1960)
- Davies, J. A., J. Denhartog, L. Eriksson, & J. W. Mayer
Can. J. of Phys. 45 4052, (1967)
- Dearnaley, G.
Report of United Kingdom Atomic Energy Authority Research Cp. Feb. 1969.
- Eriksson, L., J. A. Davies, J. Denhartog, J. W. Mayer, O. J. Marsh, &
P. Mankarious
Appl. Phys. Letters 10 323, (1967)
- Fermi, E.
Z. Physik 48 73, (1928)
- Firsov, O. B.
Sov. Phys. JETP 9 1076, (1959)
- Gibbons, J. F.
Proc. of IEEE 56 #3 (1968)
- Johnson, W. S. & J. F. Gibbons
LSS Projected Range Statistics in Semiconductors
distributed by Stanford Univ. Bookstore (1969)
- Kalbitzer, S., R. Bader, H. Herzer & K. Bethge
Z. fur Physik 203 117, (1967)

- Kellett, C. M., W. J. King, F. A. Leith et al
 "High Energy Implantation of Materials."
 Scientific Report 1 May 1966
 Ion Physics Corp. Burlington, Mass.
- Kerr, J. A. & L. N. Large
 New Scientist 39 514, (1968)
- King, W. J., J. T. Burrill, S. Harrison, F. Martin, & C. M. Kellett
 Nucl. Instr. Meth. 38 178, (1965)
- Kleinfelder, W. J., W. S. Johnson & J. F. Gibbons
 Can. J. of Phys. 46 597, (1968)
- Laegsgaard, E., F. W. Martin & W. M. Gibson
 IEEE - Trans. Nucl. Sci. NS-15 #3 239-45 June 1968
- Lehmann, C. & G. Liebfried
 J. Appl. Phys. 34 2821, (1963)
- Lindhard, J. & M. Scharff
 Phys. Rev. 124 128, (1961)
- Lindhard, J., M. Scharff, & H. E. Schiott
 Kgl. Danske Vid. Sels., Matt.-Fys. Medd. 33 #14 (1963)
- Lindhard, J.
 Kgl. Danske Vid. Selsk. Matt.-Fys. Medd. 34 #14 (1965)
- Mankarious, R. G., R. S. Ying, R. W. Bower, & D. L. English
 Proc. Int. Electron. Devices Meeting Boston, Oct. 1967
- Mazey, D. J., R. J. Nelson, & R. J. Barnes
 Phil. Mag. 17 1145, (1968)
- Meyer, O.
 IEEE Trans. on Nucl. Sci. NS-15 #3 232 (1968)
- Moyer, J. W.
 U. S. Patent #2,842,466 (1958)
- Nelson, R. S. & D. J. Mazey
 Can. J. of Phys. 46 689, (1968)
- Northcliffe, L. C.
 Ann. Rev. of Nucl. Sci. 13 67, (1963)
- Ohl, R.
 U. S. Patent #2,750,541 (1956)
- Owen, R. E. & M. L. Awcock
 IEEE Trans. on Nucl. Sci. NS-15 #3 290, (1968)

- Fehl, R. H., E. S. Goulding, D. A. Landis & M. Lenzlinger
"Accurate Determination of the Ionization Energy in Semiconductor Detectors."
p. 19-36 of Semiconductor Nuclear-Particle Detectors and Circuits
publication 1593 of the Nat. Academy of Sci. (1969)
- Powers, D. & W. Whaling
Phys. Rev. 126 61, (1962)
- Rourke, F. M., J. C. Sheffield, & F. A. White
Rev. Sci. Instr. 32 455, (1961)
- Shockley, W.
U. S. Patent #2,787,564 (1957)
- Smith, R. A.
Semiconductors, Cambridge University Press, (1959)
- Testerman, L.
Classified Calculations of Differential Scattering Cross Sections for Various Screened Potentials. M. S. Thesis, Physics Dept. Kansas State University, (1969)
- Thomas, L.
Proc. Cambridge Phil. Soc. 23 542, (1927) .
- van Buren, H. G.
Imperfections in Crystals, North Holland, (1960)

BORON AND PHOSPHORUS IMPLANTATION IN SILICON

by

J. DAVID SCHNEIDER

B. S., University of Missouri-Rolla, 1968

AN ABSTRACT OF A MASTER'S THESIS

submitted in partial fulfillment of the

requirements for the degree

MASTER OF SCIENCE

Department of Physics

KANSAS STATE UNIVERSITY
Manhattan, Kansas

1970

Large area regions on silicon wafers were uniformly implanted with 25-60 keV boron and phosphorus ions. Tests were then run to determine the electrical properties of these implanted crystals. Variations were made in the surface preparation, impurity doping levels, annealing temperatures and environments. Contacts were made both by using heavy (high dose) implants, and by evaporation of aluminum films onto the surface. The completed devices did not function in the intended manner as position sensitive particle detectors; apparently because of the non-ohmic contacts made to the implanted regions of the silicon.